

**REACTIVE OXYGEN SPECIES MEDIATE p53 ACTIVATION AND APOPTOSIS INDUCED BY SODIUM
NITROPRUSSIDE IN SH-SY5Y CELLS*.**

Simone Cardaci[§], Giuseppe Filomeni[§], Giuseppe Rotilio and Maria R. Ciriolo[#]

Department of Biology, University of Rome “Tor Vergata”, Via della Ricerca Scientifica, 1, I-00133 Rome, Italy (S.C., G.F., G.R., M.R.C.); and Research Centre IRCCS San Raffaele “La Pisana”, Via dei Bonacolsi, I-00163 Rome, Italy (G.F., G.R., M.R.C.).

Running title: Oxidative stress in p53 activation and SNP-induced apoptosis

#Address correspondence to:

Maria R. Ciriolo, Department of Biology, University of Rome “Tor Vergata”, Via della Ricerca Scientifica, 00133 Rome, Italy. Phone: +39 06 7259 4369 Fax: +39 06 7259 4311.

e-mail: ciriolo@bio.uniroma2.it

text pages: 32

number of figures: 7 + 1 supplemental

number of references: 37

number of words in Abstract: 250

Introduction: 465

Discussion: 1312

ABBREVIATIONS:

AMS, ammonium sulfamate; DCFH-DA, 2',7'-dichlorodihydrofluorescein diacetate; DMSO, dimethyl sulfoxide; DEF; deferoxamine mesylate; DMTU, dimethyl thiourea; TEMPOL, 4-hydroxy-2,2,6,6-tetramethylpiperidine-N-oxyl; DNP, 2,4-dinitrophenylhydrazine; GSH, reduced glutathione; GSSG, glutathione disulfide; NO, nitric oxide; NO_x, nitrites and nitrates; PARP, poly ADP ribose polymerase; RNS, reactive nitrogen species; ROS, reactive oxygen species; SNP, sodium nitroprusside; SNP_{ex}, photo-exhausted SNP; zVAD-fmk, benzyloxycarbonyl-Val-Ala-Asp-fluoromethyl ketone

ABSTRACT

Sodium nitroprusside (SNP) is a water soluble iron nitrosyl complex clinically used as a powerful vasodilator for treatment of hypertension and, in basic research, to mainly investigate the cytotoxic effects of nitrosative stress. Although nitric oxide (NO) is considered a pharmacologically active molecule, not all the biological effects of SNP are dependent on its NO moiety. In order to elucidate the molecular executioner(s) responsible for SNP cytotoxicity, this study determines the involvement of oxidative stress in p53 activation and apoptotic induction elicited by SNP in SH-SY5Y neuroblastoma cells. We demonstrate that pro-apoptotic activity of SNP is independent on NO production, because SNP and its two-day light exhausted compound (SNP_{ex}) trigger apoptosis at the same extent. We provide evidence for the occurrence of oxidative stress and oxidative damages during both SNP and SNP_{ex} exposure and demonstrate that iron-derived reactive oxygen species (ROS) are the genuine mediators of their cytotoxicity. We show that p53 is equally activated upon both SNP and SNP_{ex} treatments. Moreover, as demonstrated by siRNA experiments, we indicate its primary role in the induction of apoptosis, suggesting the ineffectiveness of NO in its engagement. The attenuation of p53 levels, obtained by oxy-radical scavengers, consistently with the recovery of cell viability and ROS decrease, demonstrate that SNP-mediated p53 activation is an event triggered by ROS and/or ROS-mediated damages. Altogether our results suggest that investigations on the physio-pathological effects of SNP should consider the role of ROS, other than NO, particularly in some conditions such as apoptotic induction and p53 activation.

INTRODUCTION

Nitric oxide (NO) is a diffusible and reactive free radical involved in a wide range of physiological functions, including the control of vascular tone, platelet aggregation and the immune response (Moncada et al., 1991; Mannick, 2006). In the central nervous system NO plays a pivotal role as neurotransmitter, neuromodulator and neuroprotector, even if alteration in its synthesis is detrimental for neuronal cell viability. In fact during its overproduction, NO acts as a pro-apoptotic molecule activating mainly the mitochondrial apoptotic pathway by modulating the expression of apoptosis-associated proteins such as Bax and Bcl-2 (Brüne, 2005; Pacher et al., 2007). Moreover, sustained production of NO and its reactive nitrogen species (RNS) lead to DNA damages promoting the activation of the tumour suppressor p53 protein which in turn can activate transcription of regulatory genes, allowing DNA repair, or programmed cell death (Brüne and Schneiderhan, 2003; Vousden and Lane, 2007).

Generally, patho-physiological processes controlled by NO and RNS are investigated by using NO donors with different half-life, chemical properties and kinetics of release. One of the most known NO-releasing drugs is the nitroferricyanide or disodium nitroprusside (SNP), $\text{Na}_2[\text{NO-Fe}(\text{CN})_5]$, a water soluble iron nitrosyl complex consisting of a ferrous ion surrounded by five cyanide moieties and a nitrosyl group. On the basis of its very short half-life, as well as of the immediate and rapid dissipation of its bioactivity, SNP has been clinically used as a powerful vasodilator for treatment of cardiac failures and all forms of hypertensive emergencies and, in basic research, to mainly investigate the apoptotic mechanisms triggered under conditions of nitrosative stress (Friederich and Butterworth, 1995; Chen et al., 1991; Li et al., 2004)

It is well documented that NO is the molecule responsible for many pharmacological and toxicological effects elicited by SNP. Nevertheless, several *in vitro* studies revealed that many other biological properties of SNP are independent on the NO moiety because of the huge number of by-products released during its decomposition, such as cyanide, iron and reactive oxygen species

which could account predominantly for SNP bioactivity. For instance, it has been recently demonstrated that the ability of SNP to induce heme oxygenase-1 expression (Kim et al., 2006) and iron regulatory protein 2 (IRP2) degradation (Wang et al., 2006) is not tightly dependent on NO release but is rather mediated by the release of its iron moiety. Moreover, it has been demonstrated that hydrogen peroxide production is implicated in SNP induced cardiomyocytes death (Rabkin and Kong, 2000) and a synergism between NO and the FeCN portion of SNP has been hypothesized to be functional for SNP-induced oligodendrocytes apoptosis (Boullerne et al., 1999).

In the attempt to elucidate the molecular mechanisms underlying SNP cytotoxicity, the current study deeply investigates the role played by oxidative stress in p53 activation and commitment of SH-SY5Y neuroblastoma cells to cell death.

MATERIALS AND METHODS

Materials

SNP was from Alexis (Lausen, Switzerland). Amonium sulfamate (AMS), dimethyl sulfoxide (DMSO), dimethylthiourea (DMTU), EDTA, EGTA, paraformaldehyde, propidium iodide, Deferoxamine mesylate (DEF), TEMPOL, thiosulfate and Triton X-100 were from Sigma (St. Louis, MO). Goat anti-mouse and anti-rabbit IgG (H+L)-horseradish peroxidase conjugate was from Bio-Rad Lab. (Hercules, CA). All other chemicals were obtained from Merck (Darmstadt, Germany).

Cell culture

Rat phaeochromocytoma PC12 cells were grown in DMEM containing 15% horse serum, 2.5% FBS and 1% penicillin/streptomycin. Human neuroblastoma SH-SY5Y and gastric adenocarcinoma AGS cell line were purchased from the European Collection of Cell Culture and grown in Dulbecco's MEM-F12 and in F12 medium respectively. Murine motor neuron \times neuroblastoma hybrids NSC34 were kindly provided by Dr. Neil R. Cashman (University of Toronto, Canada) and grown in DMEM. Except for PC12, all other cell media were all supplemented with 10% fetal calf serum (FCS), 1% penicillin/streptomycin and 1% glutamine. The cells were maintained at 37° C in a 5% CO₂ atmosphere in air and routinely trypsinized, plated at 4 x 10⁴/ cm² flasks. Cell viability was assessed by Trypan blue exclusion.

Treatments

A 0.5 M solution of SNP or Fe(CN)₆ (Merck) was prepared just before the experiments by dissolving the powders in water. Treatments were performed at final concentrations ranging from 0.5 to 2 mM, in medium supplemented with serum. As control, equal volumes of water were added to untreated cells. Exhausted SNP (SNP_{ex}) was obtained by leaving the solution of SNP under light exposure for two days at room temperature as previously reported (Wang et al., 2006). 2 mM of SNP or SNP_{ex} was selected for all the experiments because it allowed to evaluate a reliable degree

of apoptosis in a time-window of 24 h, and because 2 mM is the concentration close to the EC_{50} of the SNP in SH-SY5Y cells. AMS was used at final concentration of 10 mM, added with SNP and maintained throughout the experiment. The pan-caspase inhibitor zVAD-fmk (Alexis) was used at a final concentration of 20 μ M, pre-incubated for 1 h before the addition of SNP or SNP_{ex} , and maintained throughout the experimental time. The cell permeable hydroxyl radical scavengers (DMTU, DMSO and TEMPOL) were used at final concentrations of 20 mM, 3 μ M and 1.5 μ M, respectively, added with SNP and maintained throughout the experiment. Similarly, the iron chelator DEF was used to reach the final concentrations of 100 μ M. 2 mM of the rhodanese substrate, thiosulfate, or 1 μ M purified antioxidant enzymes catalase or superoxide dismutase were added 1 h before SNP addition and maintained in the medium throughout the experimental time.

Analysis of cell viability and apoptosis

Adherent (after trypsinization) and detached cells were combined, washed with PBS and stained with 50 μ g/ml propidium iodide prior to analysis by a FACScalibur instrument (Becton Dickinson, San Josè, CA). The percentages of apoptotic cells were evaluated according to Nicoletti et al. (Nicoletti et al., 1991) by calculating peak area of hypodiploid nuclei (SubG1).

Measurement of nitrite and nitrate concentration

NO released from SNP was indirectly quantified by measuring the oxidation by-products nitrites and nitrates (NO_x). Analyses of NO_x concentration were done either in water or cell media by the reaction with the Griess reagent according to Kotsonis *et al.* (Kotsonis et al. 1999). Total NO_x were measured upon nitrate reductase-mediated reduction of nitrates. The concentration of NO_x was determined by a standard curve obtained with known amount of sodium nitrite and expressed as μ M.

Western blot analyses

Total protein extracts were obtained by rupturing cells with 30 min of incubation on ice in lysis buffer (50 mM Tris-HCl, pH 7.4, 1 mM EDTA, 1 mM EGTA, 1% Triton X-100, 10 mM NaF, 1

mM sodium orthovanadate) and protease inhibitor cocktail (Roche Applied Science, Monza, Italy) followed by centrifugation at $22,300 \times g$ for 20 min at 4°C. Protein extracts were then separated by SDS-PAGE and blotted onto nitrocellulose membrane (Bio-Rad). Monoclonal anti-p53 (clone BP5312), anti-actin (Sigma), anti-procaspase-3 (clone3G2 – Cell Signaling Technology, Beverly, MA), anti-poly-ADP ribose polymerase (PARP) (Santa Cruz Biotechnology, Santa Cruz, CA), anti-Hsp90 (BD-Transduction Laboratories, Franklin Lakes, NJ); and polyclonal anti-p21, anti-Bax (Santa Cruz Biotechnology), anti-procaspase-9 (Cell Signaling Technology) were used as primary antibodies. The specific protein complex, formed upon specific secondary antibody treatment, was identified using a Fluorchem Imaging system (Alpha Innotech, Analitica De Mori, Milano, Italy) after incubation with ChemiGlow chemiluminescence substrate (Alpha Innotech).

Measurement of glutathione, ROS levels and carbonylated proteins

Intracellular reduced (GSH) and oxidized (GSSG) forms of the tripeptide glutathione were assayed upon formation of S-carboxymethyl derivatives of free thiols with iodoacetic acid, followed by the conversion of free amino groups to 2,4-dinitrophenyl derivatives by the reaction with 1-fluoro-2,4-dinitrobenzene as previously described (Filomeni et al., 2003a) Detection of intracellular ROS by 2',7'-dichlorodihydrofluorescein diacetate (DCFH-DA, Invitrogen-Molecular Probes), was performed as previously described (Filomeni et al., 2003b). Carbonylated proteins were detected using the Oxyblot Kit [Intergen (Purchase, NY)] after reaction with 2,4-dinitrophenylhydrazine (DNP) for 15 min at 25 °C. Samples were then resolved by 10% SDS-PAGE and DNP-derivatized proteins were identified by immunoblot using an anti-DNP antibody (Filomeni et al., 2007).

Fluorescence microscopy analyses

Cells were plated on chamber slides at $6 \times 10^4/\text{cm}^2$, fixed with 4% paraformaldehyde and permeabilized. Afterward, they were washed exhaustively with PBS, blocked with PBS containing 10% FCS, incubated with a monoclonal anti-ser-139-phosphorylated histone H2A.X antibody (clone JBW301 – Upstate Biotechnology, Lake Placid, NY), in combination with a polyclonal anti-p53 antibody (Sigma) and further probed with Alexa fluor[®]-488 and Alexa fluor[®]-568-conjugated

secondary antibodies (Invitrogen-Molecular Probes), respectively. To visualize nuclei, cells were also incubated with the cell permeable DNA dye Hoechst 33342 (Calbiochem-Novabiochem), washed with PBS and analyzed by fluorescence microscopy.

To evaluate mitochondrial integrity, cells were stained with 50 nM of the mitochondrial transmembrane potential ($\Delta\Psi_{mit}$)-sensitive probe MitoTracker Red[®] (Invitrogen-Molecular Probes), washed and analyzed cytofluorometrically or, alternatively, fixed with 4% paraformaldehyde and analyzed by fluorescence microscopy.

Images of cells were digitized with a Cool Snap video camera connected to Nikon Eclipse TE200 fluorescence microscopy. All images were captured under constant exposure time, gain and offset.

Iron determination

Cell pellets were diluted 1:2 with 65% HNO₃. After 1 week at room temperature, iron concentration was measured by atomic absorption spectrometry using an AAnalyst 300 Perkin-Elmer instrument, equipped with a graphite furnace with platform HGA-800 and an AS-72 auto sampler.

siRNA transfections

Twenty-four hours after plating, 50% confluent SH-SY5Y cells were transfected, with a 21-nucleotide siRNA duplex directed against the p53 mRNA target sequence, 5'-GACUCCAGUGGUAUAUCUACTT-3' (sip53) (MWG Biotech, Ebersberg, Germany). Control cells were transfected with a scramble siRNA duplex, which does not present homology with any other human mRNAs (siScr). Cells were transfected by electroporation using a Gene Pulser Xcell system (Bio-Rad) according to the manufacturer's instructions and immediately seeded into fresh medium. Transfection efficiency of siRNA into SH-SY5Y cells was estimated by co-transfecting p53 siRNA with non-specific rhodamine-conjugated oligonucleotides and found to be > 80 %.

Protein determination

Proteins were determined by the method of Lowry et al. (Lowry et al., 1951).

Data presentation

All experiments were done at least three different times unless otherwise indicated. Data are

expressed as means \pm S.D. and significance was assessed by Student's *t* test corrected by Bonferroni's method. Differences with *p* values < 0.05 were considered significant. In particular: *, $p < 0.05$; **, $p < 0.01$; ***, $p < 0.001$.

RESULTS

SNP induces caspase-dependent apoptosis in SH-SY5Y cells

Although NO is considered the active component of SNP, growing reports indicate that several SNP-elicited cellular effects are NO-independent (Kim et al., 2006; Wang et al., 2006). To investigate the genuine mediators of neurotoxic effects triggered by SNP exposure, we treated SH-SY5Y cells, which have been previously demonstrated to be sensitive to NO-induced programmed cell death (Ciriolo et al., 2000), with different concentrations of SNP ranging from 0.5 to 2 mM. **Fig. 1A** shows cytofluorometric analyses of SH-SY5Y cells treated with SNP for 24 h: plots displayed a dose-dependent increase in the percentage of apoptotic and G2/M phase blocked cells. These data are in agreement with results previously obtained on SH-SY5Y treated with the same concentrations of SNP (Ghatan et al., 2000; Feng et al., 2002; Li et al., 2004). We then evaluated whether SNP treatment triggered a caspase-dependent apoptotic process by means of the activation of the mitochondrial pathway. **Fig. 1B** shows that 12 h treatment with SNP induced a significant decrease of pro-caspase-9 and pro-caspase-3 immunoreactive bands. This event was associated with the proteolysis of poly-ADP ribose polymerase (PARP). To confirm the occurrence of a caspase-mediated apoptotic response upon SNP treatment, we incubated the cells for 1 h with the pan-caspase inhibitor zVAD-fmk before the addition of SNP, and measured cytofluorometrically the apoptotic extent after 24 h of treatment. **Fig. 1C** shows that cell viability was recovered by inhibiting caspases activation confirming that caspase-mediated apoptosis was the principal mechanism of cell death induction in our experimental conditions.

Thus, in order to evaluate a correlation between apoptosis commitment and NO release, we analyzed the concentration of nitrites and nitrates (NO_x) produced in cell medium up to 24 h of SNP

treatment. **Fig. 1D** shows that addition of SNP to culture media induced a time and dose-dependent increase in the NO_x levels suggesting that SNP toxicity could be related to NO production.

Apoptotic induction is not related to NO and cyanide moieties of SNP

To verify a direct causative role of NO moiety in the apoptotic process, we incubated SH-SY5Y cells with the two-day photo-degraded SNP (SNP_{ex}), which corresponds to its derived NO-exhausted compound (Wang et al., 2006). Surprisingly, histograms depicted in **Fig. 2A** shows that SNP_{ex} still induced apoptosis with the same trend of the freshly prepared SNP, demonstrating that NO is not the exclusive molecule involved in the induction of apoptosis in SH-SY5Y cells.

To assess whether incomplete photo-degradation of SNP could account for the similar effects of SNP and SNP_{ex} on cell viability, we verified the effective NO-exhaustation by analyzing the kinetic of NO_x production. **Fig. 2B** shows that the content of NO_x , obtained after dissolving 2 mM SNP in water or cell medium under condition of light exposure increased up to two days after which a plateau was reached that remained almost unchanged during the following seven days.

Results obtained showed that the levels of NO_x were higher (about one-fold) in water than in cell medium, likely owing to the presence of proteins and supplements able to react with NO, thus avoiding its oxidation into nitrites and nitrates. This was however in line with data reported by other authors demonstrating that two days of light exposure allows SNP to release all the available NO (Wang et al., 2006; Rauhala et al., 1998). Indeed, **Fig. 2C** shows that, unlike from what observed with freshly-prepared SNP, the concentration of NO_x measured in the medium of cells treated with the photo-degraded SNP did not change significantly during 24 h treatment, demonstrating that the drug was effectively NO exhausted.

Increasing data from literature demonstrate that nitrite is a bioactive oxidation product of NO able to elicit physio-pathological effects both in *in vivo* and in *in vitro* systems (Wink et al., 2001; Cosby et al., 2003). We then evaluated whether NO_x , mainly nitrites generated by SNP under light exposure, could be involved in the cell death process. To evaluate this possibility, we co-treated the cells for 24 h with SNP or SNP_{ex} along with the nitrite scavenger ammonium sulfamate (AMS) and

analyzed cytofluorimetrically the apoptotic extent. **Fig. 2D** shows that treatment of cells with AMS did not protect cells from SNP or SNP_{ex}-induced apoptosis, demonstrating that nitrites are not involved in the apoptotic commitment.

Overall the results clearly demonstrate that neither the NO moiety, nor NO bioactive degradation product nitrite affect cell viability in SH-SY5Y, suggesting that other molecule(s) could be responsible for apoptotic induction elicited by SNP treatment.

We analyzed if the vulnerability of SH-SY5Y cells towards SNP was a feature shared with other neuronal cell lines. Therefore, we selected two cell lines known to be sensitive to NO toxicity such as the murine motor neuron × neuroblastoma hybrid NSC34 and the rat pheochromocytoma PC12. We treated the cells with different concentrations of the freshly prepared or light-exhausted SNP and measured cytofluorimetrically the extent of apoptosis. **Fig. 2E** shows that PC12 and NSC34 cells displayed an higher degree of sensitivity towards SNP toxicity with respect to SH-SY5Y, but they are equally sensitive to both fresh and photo-degraded SNP.

Besides the generation of NO and its derived metabolites, solubilization of SNP leads to the production of free cyanide (CN⁻) (Friederich and Butterworth, 1995) that could, at least in part, account for apoptosis induction (Mills et al., 1996; Shou et al., 2003). To exclude the possibility that CN⁻ contributed to SNP cytotoxicity we monitored mitochondria integrity by labeling these organelles with the trans-membrane potential-sensitive probe MitoTracker Red[®]. Results obtained (see **Supplemental Figure 1**) demonstrate that mitochondria of cells treated for 12h with SNP, were unaffected by SNP. Moreover, incubation with thiosulphate, the substrate used by rhodanese in CN⁻ detoxification did not decrease apoptosis extent (see **Supplemental Figure 1**), indicating that free CN⁻ has not a primary role in SNP-mediated cytotoxicity.

ROS produced by SNP are responsible for SH-SY5Y cell death

To deeply dissect the NO-independent mechanism(s) underlying SNP-mediated cell death, we focused on the capability of SNP to induce oxidative stress. Indeed, it has been demonstrated that

both during its redox cycling (Ramakrishna Rao and Cederbaum, 1996) and after NO release (Rahuala et al., 1998), SNP is able to trigger the generation of reactive oxygen species (ROS), mainly hydroxyl radical (OH \cdot) *via* Fenton reaction. On the basis of these data, we measured cytofluorimetrically ROS content by incubating the cells with the ROS-sensitive fluorochrome 2',7'-dihydrodichlorofluorescein diacetate (DHDCF-DA). **Fig. 3A** shows that ROS were efficiently and time-dependently produced already at 3 h of SNP treatment. These results prompted us to analyze the content of the tripeptide glutathione, the main and the most abundant low molecular weight antioxidant in the cell, by monitoring the alterations in the concentration of both its reduced (GSH) and oxidized (GSSG) forms. HPLC analyses show that GSH decreased at 3 h from SNP addition to rise time dependently up to 12 h (+ 64.3 \pm 1.2%) (**Fig. 3B**). GSSG increased during treatment and accumulated within the cells whereas no detectable changes in the concentration of mixed disulfides between proteins and GSH (*S*-glutathionylated proteins) could be evidenced (data not shown). Conversely, the amount of carbonylated proteins rose up in a time-dependent manner (**Fig. 3C**), mirroring the kinetics of ROS and GSSG production, indicating that a sustained oxidative stress takes place upon SNP treatment. Since a sustained exposure to ROS could induce DNA damages resulting in double strand ruptures, we then monitored if SNP treatment could affect DNA integrity. We analyzed the phospho-activation of the DNA double strand break-sensitive histone H2A.X by fluorescence microscopy. **Fig. 3D** shows that SNP treatment resulted in the appearance of discrete nuclear *foci* at 6 h, which increased significantly after 12 h. The pictures indicates the recruiting sites of the DNA repair machinery and revealed a DNA-specific damage, occurring, also in this case, in a time-dependent manner. Moreover, since SNP is an iron-nitrosyl complex and iron is a redox active metal which represents an excellent catalyst of redox cycles, we determined intracellular iron accumulation by means of atomic absorption spectroscopy. **Fig. 3E** shows that iron accumulated intracellularly in a time-dependent manner reaching values close to 3 nmoles Fe/mg protein at 12 h of treatment, values similar to those obtained upon treatment with SNPex (data not shown). We then performed experiments with deferoxamine mesylate (DEF), a

well known iron chelator, and cytofluorometrically analyzed ROS content and apoptosis. Cells incubated for 3 h with SNP or SNP_{ex} in the presence of DEF showed a significant decrease of ROS concentration to values similar to untreated cells (**Fig. 3F**). This result well correlated with the percentage of apoptotic cells measured after 24 of treatment with SNP or SNP_{ex} (**Fig. 3F**), confirming the role of iron as principal ROS generator under our conditions. To establish the role of ROS as functional mediator of SNP-, as well as of SNP_{ex}-induced apoptosis we tested the effect of several antioxidants and ROS scavengers on SH-SY5Y viability. Incubation of the cells with specific OH[•] radical scavengers such as DMTU, DMSO and TEMPOL, resulted in a significant protection against SNP- and SNP_{ex}-induced apoptosis (**Fig. 4A**). By contrast, no significant recovery of cell viability was achieved by treating the cells with superoxide dismutase or catalase, enzymes catalyzing the scavenging of superoxide and hydrogen peroxide, respectively (data not shown). To verify the effective antioxidant ability of DMTU, DMSO and TEMPOL, we measured ROS production during their incubation along with SNP and SNP_{ex}. Consistently with the recovery of cell viability, these radical scavengers reduced ROS concentration (**Fig. 4B**). These overall data demonstrate that ROS represent the molecular inducers of SNP cytotoxicity suggesting that OH[•] is likely the oxy-radical principally involved in the apoptotic induction.

Involvement of p53 in SNP cytotoxicity

To dissect the signaling pathway(s) involved in SNP-induced apoptosis, we focused on p53, a transcription factor activated by several stress conditions such as redox unbalance and DNA damage. **Fig. 4C** shows Western blot analyses of p53 upon treatment with either SNP or SNP_{ex}, evidencing an induction of the protein starting as early as 6 h of treatment to reach the highest levels after 12 h. It is worth to note that besides an enhancement of the total immunoreactivity band of p53, an increase of the high molecular weight band, reasonably representing the hyper phosphorylated/activated form of the protein (Filomeni et al., 2007) could be observed upon both treatments. To confirm p53 activation, we monitored the levels of the cyclin-dependent kinase

inhibitor p21, as well as Bax, two of the well established target genes of p53, deputed to cell cycle arrest and apoptosis commitment, respectively. As depicted by **Fig. 4C**, p21 and Bax are up-regulated after 6h of treatment suggesting that accumulation of p53 is followed by the acquisition of its nuclear trans-acting properties. To exclude the possibility that nitrite, could account for p53 activation, we co-treated the cells for 12 h with SNP or SNP_{ex} and AMS. **Fig. 4D** shows that AMS did not affect p53 activation elicited by SNP or SNP_{ex} treatment, confirming that nitrite is not involved in the activation of p53 tumor suppressor protein.

To establish the role of p53 in the apoptosis induction, we transfected SH-SY5Y cells with a siRNA against p53 (sip53) or with a scramble sequence that does not share homology with any other human mRNAs (siScr). Cytofluorimetric analyses showed that the percentage of apoptotic cells was significantly reduced upon p53 interference in both SNP and SNP_{ex} treated cells (**Fig. 4E**), demonstrating that p53, activated in response to cell damage, contributes to the apoptotic commitment. In line with such results, Western blot analyses depicted in **Fig. 4F** show that p53, as well as its downstream targets, Bax and p21 were only slightly induced upon 6 and 12 h of treatment with SNP and SNP_{ex} in sip53 cells with respect to siScr counterparts.

Data presented so far demonstrated that SNP treatment was able to produce sustained oxidative stress and cellular damages which culminated in cell death and elicited p53 activation regardless NO production. Nevertheless, a direct link between ROS production and p53 induction was not pointed out yet. Therefore, to directly examine the role of ROS in p53 activation, we treated SH-SY5Y cells with DMTU, DMSO and TEMPOL along with SNP or SNP_{ex}. **Fig. 5A** show that, similarly to the recovery of cell viability (**Fig. 4A**) and scavenge of ROS (**Fig. 4B**), DMTU, DMSO and TEMPOL reduced p53, p21 and Bax accumulation after 12h of treatment, demonstrating that in our experimental system, p53 activation was a ROS-dependent event. Moreover, thiosulphate incubation did not affect p53 induction (see **Supplemental figure 1**), confirming that CN⁻ did not contribute to SNP pro-apoptotic activity. The functional connection between ROS, nuclear damage and p53 activation was further revealed by means of fluorescence microscopy. As depicted in **Fig.**

5B, DMTU, DMSO and TEMPOL were able to reduce the phospho-activation levels of the histone H2A.X after 12h of treatment with SNP, as well as p53 nuclear localization (**Fig. 5B**), providing a link between oxidative stress, DNA damage and the engagement of p53-mediated signaling pathway.

Ferricyanide is unable to reproduce SNP-mediated toxic effects

To further validate the primary role played by ROS in SNP-induced p53 activation and apoptosis, we treated SH-SY5Y cells with ferricyanide $[\text{Fe}(\text{CN})_6]$, the structurally closest and most stable analogue of SNP, often used as its sham control. Lacking of any NO moiety, $\text{Fe}(\text{CN})_6$ is unable to produce NO, but differently from SNP_{ex} , it is a redox steady molecule. In fact, as shown in **Fig. 6A**, treatment with $\text{Fe}(\text{CN})_6$ did not rise up intracellular ROS concentration even after 12 h of treatment, confirming the different redox nature of SNP_{ex} and $\text{Fe}(\text{CN})_6$, with the former able to catalyze ROS production and the latter completely inert. Consistently with this feature, $\text{Fe}(\text{CN})_6$ was neither able to affect SH-SY5Y cells viability (**Fig. 6B**) nor effective in inducing p53 up-regulation (**Fig. 6C**), providing further evidences that SNP-induced cell death and p53 activation are two phenomena elicited by a ROS-mediated insult.

ROS resistant cells are insensitive to SNP-induced cell damage and apoptosis

To deeply investigate the role of oxidative stress as the main mediator in SNP-induced apoptosis and p53 activation, we selected the gastric adenocarcinoma AGS, a cell line known to be particularly resistant to ROS-mediated damages and death by means of its efficient antioxidant systems, mainly associated with GSH and its related enzymes (Filomeni et al., 2005). **Fig. 7A** shows histograms from analyses of apoptotic cells indicating that AGS cells did not undergo cell death upon 24 h of treatment with 2 mM SNP, although the amount of NO_x generated was comparable between the two cell lines (142.30 ± 25.12 versus 119.90 ± 4.20 in AGS and SH-SY5Y respectively). Moreover, SNP treatment did neither elicit a significant increase of protein carbonyls

(**Fig. 7B**), nor an appreciable DNA damage (**Fig. 7C**). Consistently with these observations, no p53 up-regulation was observed up to 12h of SNP treatment (**Fig. 7D**), confirming the hypothesis that SNP toxicity and p53 activation are directly linked to cellular sensitivity to oxidative stress.

DISCUSSION

This paper demonstrates that ROS, rather than NO, are the genuine mediator of apoptosis elicited upon SNP exposure in SH-SY5Y cells, in line with growing evidences showing other effectors of SNP bioactivity. In fact, no difference was observed in the apoptotic cell percentage between freshly prepared and SNP_{ex}, which is devoid of NO. SNP exhaustion can be triggered by light exposure, as well as by reductive processes carried out in an enzymatic or thiol-mediated fashion (Rao et al., 1991; Mohazzab-H et al., 1999; Grossi and D'Angelo, 2005) during which the nitroprusside nitroxide radical anion undergoes redox cycling to generate hydroxyl radical (OH[•]) (Ramakrishna Rao and Cederbaum, 1996). Moreover, Rauhala et al. demonstrated that the ability of SNP to generate ROS is further maintained after the complete release of NO by means of the free iron coordination site for H₂O₂ that can lead to the generation of OH[•] via the Fenton reaction (Rauhala et al., 1998). In line with these observations, we demonstrate the occurrence of an oxidative stress and cellular oxidative damages during both SNP and SNP_{ex} exposure in SH-SY5Y cells. Although an indirect ROS production was already pointed out in several papers describing pro-apoptotic properties of NO-donors (Pacher et al., 2007), the pro-oxidant action of SNP seems to be an intrinsic characteristic of this molecule. In fact, whereas NO and RNS can increase intracellular ROS content, e.g. by inhibiting components of the mitochondrial respiratory chain (Schild et al., 2003), we found that SNP is able to directly induce apoptosis and generate ROS proportionally to its concentration (data not shown) and independently on mitochondria impairment. Moreover, the recovery of cell viability and the consistent attenuation of ROS formation, obtained using radical scavengers relatively specific for OH[•], demonstrate that ROS, generated upon SNP decomposition, could be the genuine mediators of its cytotoxicity. Moreover, the ineffectiveness of SOD and catalase in decreasing SNP toxicity supports the hypothesis that OH[•] is reasonably the main oxy-radical involved in the induction of apoptosis.

The pivotal role played by ROS in SNP cytotoxicity was also confirmed by the experiments carried out with $\text{Fe}(\text{CN})_6$. This compound is structurally the closest analogue of SNP, in which the NO moiety is replaced by another cyanide group but, notwithstanding their structural similarity, they exhibit different stability and reactivity remaining distinct iron containing molecules, with $\text{Fe}(\text{CN})_6$ being a ROS unproductive molecule. These properties can reasonably explain the different effects observed on SH-SY5Y cells viability, where $\text{Fe}(\text{CN})_6$ was not toxic. Moreover these results strengthen the role played by ROS in SNP-induced apoptosis and, at the same time, as previously suggested in other reports (Rauhala et al., 1998; Wang et al., 2006), indicate in SNP_{ex} a more suitable control compound to assess the molecular effectiveness of SNP bioactivity, with respect to $\text{Fe}(\text{CN})_6$. The involvement of ROS in cell demise supports the hypothesis that p53 could be activated in response to ROS-dependent nuclear damages and could mediate the induction of apoptosis. p53 is one of the most characterized tumor suppressor protein which acts in response of different forms of cellular insults such as hypoxia, DNA damage, oxidative and nitrosative stress to mediate a variety of anti-proliferative processes, among which the control of cell cycle and apoptosis (Vousden and Lane, 2007). According to the current view, phosphorylation of p53 at various sites, increases its stabilization and nuclear accumulation in nuclei where it coordinates different responses to stress signals, by modulating the expression of a wide group of target genes, among which p21 and Bax are two of the best characterized. In response to DNA damage, p53 promotes cell cycle arrest at G1 or G2 phase to allow DNA to be repaired before proceeding into mitosis, by inducing the expression of cyclin-dependent kinases inhibitors such as p21. When the damage is too severe to be repaired, p53 also regulates the expression of several genes (e.g. Bax) able to engage mitochondrial apoptotic pathway leading to cell death (Yu and Zhang, 2005; Fridman and Lowe, 2003). In line with the general understanding of p53 regulation, in the current study we report that SNP treatment is able to trigger p53 phospo-activation and nuclear accumulation which stand for the acquisition of transcriptional activity as evidenced by the increase of p21 and Bax levels. Whereas up-regulation of p21 is consistent with cell cycle arrest in G2/M

phase, event particularly evident with intermediate doses of SNP, Bax induction could be functional to mediate the pro-apoptotic activity of p53, as demonstrated by the attenuation of the apoptotic extent in experiments performed with p53 siRNA. The engagement of both p53/p21 and p53/Bax signaling pathways appears to be triggered by ROS and/or ROS-mediated damages during SNP treatment: in fact, oxy-radical scavengers attenuate DNA double strand breaks, p53 activation and p21/Bax up-regulation as well. The role played by ROS in apoptotic induction and p53 activation finds further confirmations in the different behaviors of neuroblastoma and AGS cells towards SNP toxicity. In a previous work, we demonstrated that the gastric adenocarcinoma AGS cells are particularly resistant to ROS-mediated insults by exploiting their efficient GSH-related antioxidant systems (Filomeni et al., 2005). Although the amount of NO_x generated by SNP was the same in the two cell lines, AGS cells are completely insensitive to SNP induced cell damages and death, reinforcing the hypothesis that SNP toxicity and p53 activation are two phenomena directly linked to cellular sensitivity to oxidative stress. It has to be pointed out that DNA damage, activation of p53 as well as p21-mediated cell cycle arrest and Bax up-regulation, are believed to play an important role during nitrosative stress and NO-induced apoptosis of various cell types, including SH-SY5Y cells (Kim et al., 2002; Ciriolo et al., 2000; Lee et al., 2006). However the fact that SNPex was efficient in generating ROS and to increase p53, p21 and Bax content as much as SNP and the ineffectiveness of AMS in reducing apoptotic degree are straightforward evidences that neither the NO moiety of SNP, nor its derived oxidation by-product nitrite, are directly involved in apoptosis induction, in our experimental conditions.

Although the biochemical mechanisms responsible for ROS production upon SNP treatment deserve to be deeply investigated, on the basis of literature data and the results obtained here, it is reasonable to suppose an active involvement of iron in oxidative stress induced by SNP. Indeed, atomic absorption spectroscopy showed that upon SNP treatment, iron accumulated intracellularly in a time-dependent manner: a result that parallels ROS increase, oxidative damages and p53 activation. Therefore, this event could reasonably represent the crucial step for the induction of

oxidative stress and let us to speculate that besides oxy-radicals, high reactive iron species such as ferryl and perferryl species $[\text{Fe(IV)=O}$ or $\text{FeO}^{2+}]$ could form as suggested in a previous work (Ramakrishna and Cederbaum, 1996), thus contributing in inducing DNA damages and accounting for SNP cytotoxicity.

Finally, we also demonstrate that upon SNP treatment, cyanide has no role in the establishment of the stress condition leading to p53 activation and cell death. In fact, although SNP contains five cyanide molecules that could promote mitochondrial impairment, our results show that mitochondria of cells treated with SNP are still viable. These results are confirmed by the maintenance of mitochondrial membrane potential, which only evidences the appearance of a small cell population at lower potential, that reasonably could be due to activation of the mitochondrial apoptotic pathway. Moreover, incubation of the cells with the highest sub-toxic concentration of thiosulphate, the substrate used by rhodanese in cyanide detoxification, does not not affect the extent of apoptosis.

Overall the results obtained in this study indicate that even though SNP represents a good NO donor in *in vivo* systems, it does not faithfully mimic patho-physiological effects elicited by NO. Therefore care is needed when interpreting studies on the effects of SNP, because the role of ROS could go beyond that of NO in some conditions, leading to misunderstandings and erroneous interpretations of results.

REFERENCES

- Boullerne AI, Nedelkoska L and Benjamins JA (1999) Synergism of nitric oxide and iron in killing the transformed murine oligodendrocyte cell line N20.1. *J Neurochem* **72**: 1050-1060.
- Brüne B (2005) The intimate relation between nitric oxide and superoxide in apoptosis and cell survival. *Antioxid Redox Signal* **7**: 497-507.
- Brüne B and Schneiderhan N (2003) Nitric oxide evoked p53-accumulation and apoptosis. *Toxicol Lett* **139**: 119-123.
- Chen J, Chang B, Williams M and Murad F (1991) Sodium nitroprusside degenerates cultured rat striatal neurons. *Neuroreport* **2**: 121-123.
- Ciriolo MR, De Martino A, Lafavia E, Rossi L, Carrì MT and Rotilio G (2000) Cu,Zn superoxide dismutase-dependent apoptosis induced by nitric oxide in neuronal cells. *J Biol Chem* **275**: 5065-5072.
- Cosby K, Partovi KS, Crawford JH, Patel RP, Reiter CD, Martyr S, Yang BK, Wacławski MA, Zalos G, Xu X, Huang KT, Shields H, Kim-Shapiro DB, Schechter AN, Cannon RO 3rd and Gladwin MT (2003) Nitrite reduction to nitric oxide by deoxyhemoglobin vasodilates the human circulation. *Nat Med* **9**: 1498-1505.
- Feng Z, Li L, Ng PY and Porter AG (2002) Neuronal differentiation and protection from nitric oxide-induced apoptosis require c-Jun-dependent expression of NCAM140. *Mol Cell Biol* **22**: 5357-5366.
- Filomeni G, Rotilio G and Ciriolo MR (2003a) Glutathione disulfide induces apoptosis in U937 cells by a redox-mediated p38 MAP kinase pathway. *FASEB J* **17**: 64-66.
- Filomeni G, Aquilano K, Rotilio G and Ciriolo MR (2003b) Reactive oxygen species dependent c-Jun NH2-terminal kinase/c-Jun signaling cascade mediates neuroblastoma cell death induced by diallyl disulfide. *Cancer Res* **63**: 5940-5949.

- Filomeni G, Aquilano K, Rotilio G and Ciriolo MR (2005) Glutathione-related systems and modulation of extracellular signal-regulated kinases are involved in the resistance of AGS adenocarcinoma gastric cells to diallyl disulfide-induced apoptosis. *Cancer Res* **65**: 11735-11742.
- Filomeni G, Cerchiaro G, Da Costa Ferreira AM, De Martino A, Pedersen JZ, Rotilio G and Ciriolo MR (2007) Pro-apoptotic activity of novel Isatin-Schiff base copper(II) complexes depends on oxidative stress induction and organelle-selective damage. *J Biol Chem* **282**: 12010-12021.
- Fridman JS and Lowe SW (2003) Control of apoptosis by p53. *Oncogene* **22**: 9030-9040.
- Friederich JA and Butterworth JF 4th (1995) Sodium nitroprusside: twenty years and counting. *Anesth Analg* **81**: 152-162.
- Ghatan S, Lerner S, Kinoshita Y, Hetman M, Patel L, Xia Z, Youle RJ and Morrison RS (2000) p38 MAP kinase mediates bax translocation in nitric oxide-induced apoptosis in neurons. *J Cell Biol* **150**: 335-347.
- Grossi L and D'Angelo S (2005) Sodium nitroprusside: mechanism of NO release mediated by sulfhydryl-containing molecules. *J Med Chem* **48**: 2622-6.
- Kim HJ, Tsoy I, Park MK, Lee YS, Lee JH, Seo HG and Chang KC (2006) Iron released by sodium nitroprusside contributes to heme oxygenase-1 induction via the cAMP-protein kinase A-mitogen-activated protein kinase pathway in RAW 264.7 cells. *Mol Pharmacol* **69**: 1633-1640.
- Kim SJ, Hwang SG, Shin DY, Kang SS and Chun JS (2002) p38 kinase regulates nitric oxide-induced apoptosis of articular chondrocytes by accumulating p53 via NFkappa B-dependent transcription and stabilization by serine 15 phosphorylation. *J Biol Chem* **277**: 33501-33508.
- Kotsonis P, Frey A, Fröhlich LG, Hofmann H, Reif A, Wink DA, Feelisch M and Schmidt HH (1999) Autoinhibition of neuronal nitric oxide synthase: distinct effects of reactive nitrogen and oxygen species on enzyme activity. *Biochem J* **340**: 745-752.
- Lee SJ, Kim DC, Choi BH, Ha H and Kim KT (2006) Regulation of p53 by activated protein kinase C-delta during nitric oxide-induced dopaminergic cell death. *J Biol Chem* **281**: 2215-2224.

- Li L, Feng Z and Porter AG (2004) JNK-dependent phosphorylation of c-Jun on serine 63 mediates nitric oxide-induced apoptosis of neuroblastoma cells. *J Biol Chem* **279**: 4058-4065.
- Lowry OH, Rosebrough NJ, Farr AI and Randall RJ (1951) Protein measurement with the Folin phenol reagent. *J Biol Chem* **193**: 265-275.
- Mannick JB (2006) Immunoregulatory and antimicrobial effects of nitrogen oxides. *Proc Am Thorac Soc* **3**: 161-165.
- Mills EM, Gunasekar PG, Pavlakovic G and Isom GE (1996) Cyanide-induced apoptosis and oxidative stress in differentiated PC12 cells. *J Neurochem* **67**(3):1039-1046.
- Mohazzab-H KM, Kaminski PM, Agarwal R and Wolin MS (1999) Potential role of a membrane-bound NADH oxidoreductase in nitric oxide release and arterial relaxation to nitroprusside. *Circ Res* **84**: 220-8.
- Moncada S, Palmer RM and Higgs EA (1991) Nitric oxide: physiology, pathophysiology, and pharmacology. *Pharmacol Rev* **43**: 109-142.
- Nicoletti I, Migliorati G, Pagliacci MC, Grignani F and Riccardi C (1991) A rapid and simple method for measuring thymocyte apoptosis by propidium iodide staining and flow cytometry. *J Immunol Meth* **139**: 271-279.
- Pacher P, Beckman JS and Liaudet L (2007) Nitric oxide and peroxynitrite in health and disease. *Physiol Rev* **87**: 315-424.
- Rabkin SW and Kong JY (2000) Nitroprusside induces cardiomyocyte death: interaction with hydrogen peroxide. *Am J Physiol Heart Circ Physiol* **279**: H3089-3100.
- Ramakrishna Rao DN and Cederbaum AI (1996) Generation of reactive oxygen species by the redox cycling of nitroprusside. *Biochim Biophys Acta* **1289**: 195-202.
- Rao DN, Elguindi S and O'Brien PJ (1991) Reductive metabolism of nitroprusside in rat hepatocytes and human erythrocytes. *Arch Biochem Biophys* **286**: 30-37.
- Rauhala P, Khaldi A, Mohanakumar KP and Chiueh CC (1998) Apparent role of hydroxyl radicals in oxidative brain injury induced by sodium nitroprusside. *Free Radic Biol Med* **24**: 1065-1073.

- Schild L, Reinheckel T, Reiser M, Horn TF, Wolf G and Augustin W (2003) Nitric oxide produced in rat liver mitochondria causes oxidative stress and impairment of respiration after transient hypoxia. *FASEB J* **17**: 2194-2201.
- Shou Y, Li L, Prabhakaran K, Borowitz JL and Isom GE (2003) p38 Mitogen-activated protein kinase regulates Bax translocation in cyanide-induced apoptosis. *Toxicol Sci* **75**: 99-107.
- Vousden KH and Lane DP (2007) p53 in health and disease. *Nat Rev Mol Cell Biol* **8**: 275-283.
- Wang J, Fillebeen C, Chen G, Andriopoulos B and Pantopoulos K (2006) Sodium nitroprusside promotes IRP2 degradation via an increase in intracellular iron and in the absence of S nitrosylation at C178. *Mol Cell Biol* **26**: 1948-1954.
- Wink DA, Miranda KM, Espey MG, Pluta RM, Hewett SJ, Colton C, Vitek M, Feelisch M and Grisham MB (2001) Mechanisms of the antioxidant effects of nitric oxide. *Antioxid Redox Signal* **3**: 203-213.
- Yu J and Zhang L (2005) The transcriptional targets of p53 in apoptosis control. *Biochem Biophys Res Commun* **331**: 851-858.

FOOTNOTES

*The work was partially supported by grants from Ministero della Salute (to M.R.C.)

§S.C. and G.F. contributed equally to this work.

LEGENDS FOR FIGURES

Figure 1. SNP induces caspase-dependent apoptosis in SH-SY5Y cells

A, SH-SY5Y cells were treated with SNP ranging from 0.5 to 2 mM for 24 h, washed and stained with propidium iodide. Analysis of subG1 (apoptotic) cells was performed by a FACScalibur instrument and percentages of staining-positive cells were calculated using WinMDI version 2.8 software. Data are expressed as % of apoptotic cells and represent the mean \pm SD of $n = 10$ independent experiments. All values are significantly different with respect to control (*Ctrl*). B, SH-SY5Y cells were treated with 2 mM SNP for different times. 50 μ g of total protein extract was loaded onto each lane for detection of pro-caspase-9, pro-caspase-3 and PARP. actin was used as loading control. Western blots are from one experiment representative of three that gave similar results. C, SH-SY5Y cells were pre-treated for 1 h with or without 20 μ M pan-caspase inhibitor zVAD-fmk, then treated with 2 mM SNP for 24 h, and analyzed for apoptosis extent. Data are expressed as % of apoptotic cells and represent the mean \pm SD of $n = 4$ independent experiments. *** $p < 0.001$. D, SH-SY5Y cells were treated with SNP ranging from 0.5 to 2 mM up to 24 h. At each time, 100 μ l of cell media were harvested and spectrophotometrically analysed for nitrite and nitrate (NO_x) content by Griess assay. Data are expressed as μ M NO_x and represent the mean \pm S.D of $n = 8$ independent experiments.

Figure 2. SNP-induced neuroblastoma apoptosis is independent on NO and NO_x production.

A, SH-SY5Y cells were treated for 24 h with different concentrations of SNP, or with equimolar amounts of two-day light degraded SNP (SNP_{ex}), and analyzed for apoptosis extent. Data are expressed as % of apoptotic cells and represent the mean \pm SD of $n = 4$ independent experiments. All values are significantly different with respect to control. B, 2 mM SNP was dissolved in water or cell medium (*DMEM/F12*) up to 9 days. The concentration of nitrite and nitrate (NO_x) produced

by SNP were measured by Griess assay. Data are expressed as $\mu\text{M NO}_x$ and represent the mean \pm SD of $n = 3$ independent experiments. *C*, SH-SY5Y cells were treated with 2 mM SNP or SNP_{ex} up to 24 h. At each time 100 μl of cell media were harvested and the concentration of NO_x measured by Griess assay. Data are expressed as $\mu\text{M NO}_x$ and represent the mean \pm SD of $n = 3$ independent experiments. *D*, SH-SY5Y cells were treated for 24 h with 2 mM SNP or SNP_{ex} with or without 10 mM ammonium sulfamate (*AMS*), and analyzed for apoptosis extent. Data are expressed as % of apoptotic cells and represent the mean \pm SD of $n = 4$ independent experiments. All values are significantly different with respect to control. *E*, NSC34 and PC12 cells were treated for 24 h with different concentrations of SNP, or with equimolar amounts of SNP_{ex} and analyzed for apoptosis extent. Data are expressed as % of apoptotic cells and represent the mean \pm SD of $n = 4$ independent experiments. All values are significantly different with respect to control.

Figure 3. SNP-induced ROS production correlates with intracellular iron uptake and oxidative damage to proteins and DNA.

A, SH-SY5Y cells were treated with 2 mM SNP for different times and cytofluorimetrically analysed for intracellular ROS content by co-incubation with 50 μM DCFH-DA. Cytofluorimetric histograms are from one experiment out of five that gave similar results. *B*, SH-SY5Y cells were treated with 2 mM SNP for different times and analyzed for intracellular levels of reduced (*GSH*) and oxidized (*GSSG*) forms of glutathione by HPLC. Data are expressed as nmoles of GSH or GSSG/mg total proteins and represent the mean \pm S.D of $n = 6$ independent experiments. *, $p < 0.05$; **, $p < 0.01$; ***, $p < 0.001$. *C*, SH-SY5Y cells were treated with 2 mM SNP for different times. 40 μg of total protein extracts were reacted with dinitrophenylhydrazine (DNP), resolved on 10% SDS-PAGE and DNP-derivatized proteins identified by Western blot using an anti-DNP antibody. Hsp90 was used as loading control and densitometry of each lane (*bottom panel*) was calculated using Quantity One Software (black bars, *control*; striped bars, *SNP-treated*). Data are

expressed as arbitrary units (a.u.) with respect to Hsp90 and represent the mean \pm S.D of $n = 4$ independent experiments. *, $p < 0.05$, **, $p < 0.01$. *D*, SH-SY5Y cells, treated with 2 mM SNP for 6 and 12 h, were used for immunofluorescence analysis of the phospho-active (ser-139) isoform of double strand break-sensitive histone H2A.X (*P-H2A.X*). Nuclear *foci* (green) stand for the recruitment of DNA repair machinery. Staining with Hoechst 33342 (blue) was performed to evidence nuclei of the cells. *E*, SH-SY5Y cells were treated with 2 mM SNP up to 12 h and analyzed for intracellular iron concentration by atomic absorption spectrometry. Data are expressed as nmoles of iron/mg total proteins and represent the mean \pm S.D of $n = 9$ independent experiments. All values are significantly different with respect to control, except for 1 h. *F*, SH-SY5Y cells were treated with 2 mM SNP or SNP_{ex}, with or without 100 μ M DEF and analyzed for intracellular ROS content, by co-incubation with 50 μ M DCFH-DA (at 3 h) or, alternatively, for apoptosis extent, upon staining with propidium iodide (after 24 h). Data are expressed as % of DCF-positive or apoptotic cells, respectively and represent the mean \pm SD of $n = 4$ independent experiments. ***, $p < 0.001$.

Figure 4. SNP-induced apoptosis is a ROS-dependent and p53-associated event.

A, SH-SY5Y cells were treated for 24 h with 2 mM SNP or two-day light degraded SNP (SNP_{ex}), with or without 20 mM DMTU, or 3 μ M DMSO, or 1.5 μ M TEMPOL, and analyzed for apoptosis extent. Data are expressed as % of apoptotic cells and represent the mean \pm SD of $n = 4$ independent experiments. *, $p < 0.05$; **, $p < 0.01$; ***, $p < 0.001$. *B*, SH-SY5Y cells were treated for 24 h with 2 mM SNP or SNP_{ex}, with or without 20 mM DMTU, or 3 μ M DMSO, or 1.5 μ M TEMPOL and cytofluorimetrically analysed for intracellular ROS content by co-incubation with 50 μ M DCFH-DA. Data are expressed as % of DCF-positive cells and represent the mean \pm SD of $n = 3$ independent experiments. ***, $p < 0.001$. *C*, SH-SY5Y cells were treated with 2 mM SNP or SNP_{ex} for different times. 50 μ g of total protein extract was loaded onto each lane for detection of p53,

p21 and Bax. Actin was used as loading control. Western blots are from one experiment representative of three that gave similar results. *P-p53*, phosphorylated p53. *D*, SH-SY5Y cells were treated for 12 h with 2 mM SNP or SNP_{ex} with or without 10 mM ammonium sulfamate (AMS). 50 µg of total protein extract was loaded onto each lane for detection of p53. Actin was used as loading control. Western blots are from one experiment representative of three that gave similar results. *E*, SH-SY5Y cells were transiently transfected with siRNA duplex directed against the p53 mRNA target sequence (sip53) or with a scramble siRNA duplex (siScr). Cell adhesion has been allowed for 12 h (time at which maximum decrease of p53 was obtained), then the cells were treated for additional 24 h with 2 mM SNP or SNP_{ex}, and analyzed for apoptosis extent. Data are expressed as % of apoptotic cells and represent the mean ± SD of n = 3 independent experiments. **, *p* < 0.01. *F*, After 12 h from cell adhesion siScr and sip53 cells were treated with 2 mM SNP or SNP_{ex} for different times. 50 µg of total protein extract was loaded onto each lane for detection of p53, p21 and Bax. Actin was used as loading control. Western blots are from one experiment representative of three that gave similar results.

Figure 5. p53 activation is responsive to SNP-induced ROS production and oxidative damage.

A, SH-SY5Y cells were treated for 12 h with 2 mM SNP, or with equimolar amounts of two-day light degraded SNP (SNP_{ex}), with or without 20 mM DMTU, or 3µM DMSO, or 1.5 µM TEMPOL. 50 µg of total protein extract was loaded onto each lane for detection of p53, p21 and Bax. Actin was used as loading control. Western blots are from one experiment representative of three that gave similar results. *P-p53*, phosphorylated p53. *B*, SH-SY5Y cells were treated for 12 h with 2 mM SNP or SNP_{ex}, with or without 20 mM DMTU, or 3µM DMSO, or 1.5 µM TEMPOL. Then the cells were used for immunofluorescence analysis of the phospho-active histone H2A.X (*P-H2A.X*, green) and p53 (red). Staining with Hoechst 33342 (blue) was performed to evidence nuclei of the cells.

Figure 6. Ferricyanide does not yield ROS increase, p53 induction and commitment to cell death.

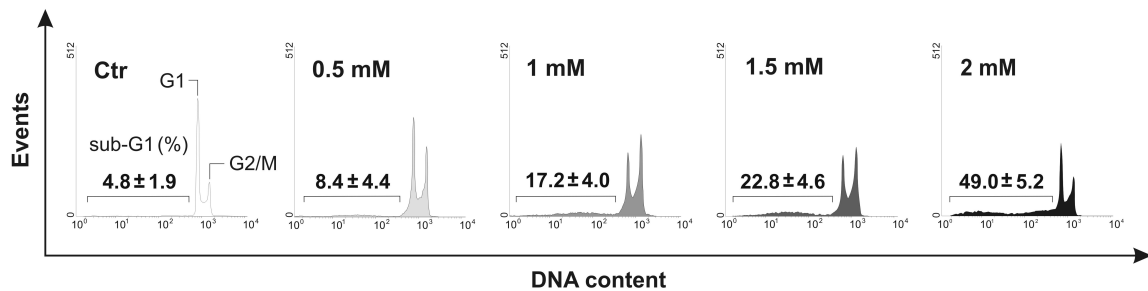
A, SH-SY5Y cells were treated for 12 h with 2 mM ferricyanide [$Fe(CN)_6$] and cytofluorimetrically analysed for intracellular ROS content by co-incubation with 50 μ M DCFH-DA. Cytofluorimetric histograms are from one experiment out of five that gave similar results (dotted line, $Fe(CN)_6$ -treated cells). B, SH-SY5Y cells were treated for 24 h with 2 mM $Fe(CN)_6$ or SNP and analysed for apoptosis extent. Data are expressed as % of apoptotic cells and represent the mean \pm SD of n = 4 independent experiments. ***, $p < 0.001$. C, SH-SY5Y cells were treated for 12 h with 2 mM $Fe(CN)_6$ or SNP. 50 μ g of total protein extract was loaded onto each lane for detection of p53. Actin was used as loading control. Western blots are from one experiment representative of three that gave similar results. P-p53, phosphorylated p53.

Figure 7. AGS cells are insensitive to SNP-mediated apoptosis.

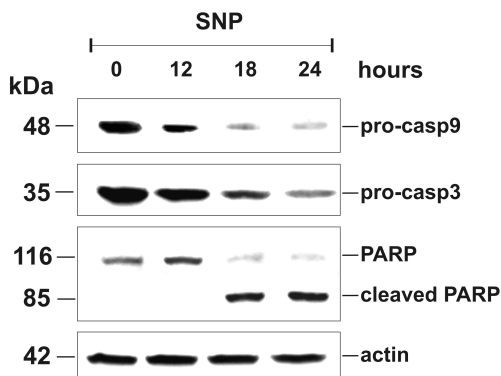
A, SH-SY5Y and AGS cells were treated with 2 mM SNP for 24 h, and analyzed for apoptosis extent. Data are expressed as % of apoptotic cells and represent the mean \pm S.D of n = 4 independent experiments. ***, $p < 0.001$. B, AGS cells were treated with 2 mM SNP for different times. 40 μ g of total protein extracts were reacted with dinitrophenylhydrazine (DNP), resolved on 10% SDS-PAGE and DNP-derivatized proteins identified by Western blot using an anti-DNP antibody. Hsp90 was used as loading control. Western blot is from one experiment representative of three that gave similar results. C, AGS cells, treated with 2 mM SNP for 12 h, were used for immunofluorescence analysis of the phospho-active histone H2A.X (P-H2A.X, green). Staining with Hoechst 33342 (blue) was performed to evidence nuclei. D, AGS cells were treated with 2 mM SNP, or with equimolar amount of two-day light degraded SNP (SNP_{ex}) for different times. 50 μ g of total protein extract was loaded onto each lane for detection of p53. Actin was used as loading

control. Western blots are from one experiment representative of three that gave similar results. *P*-*p53*, phosphorylated p53.

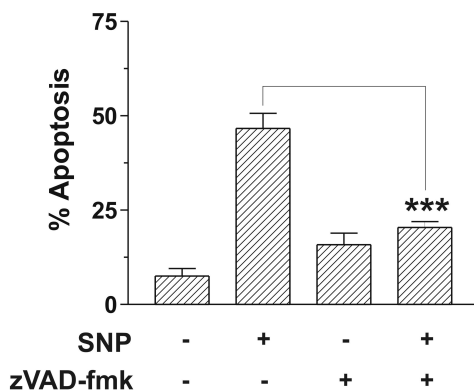
A



B



C



D

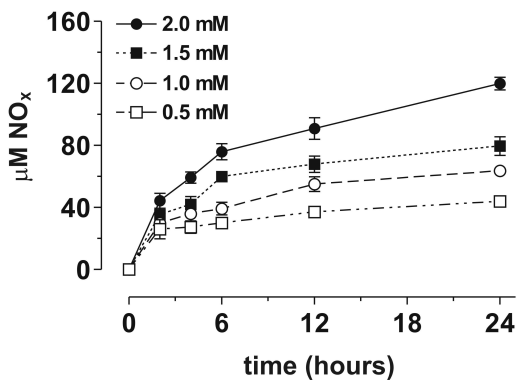


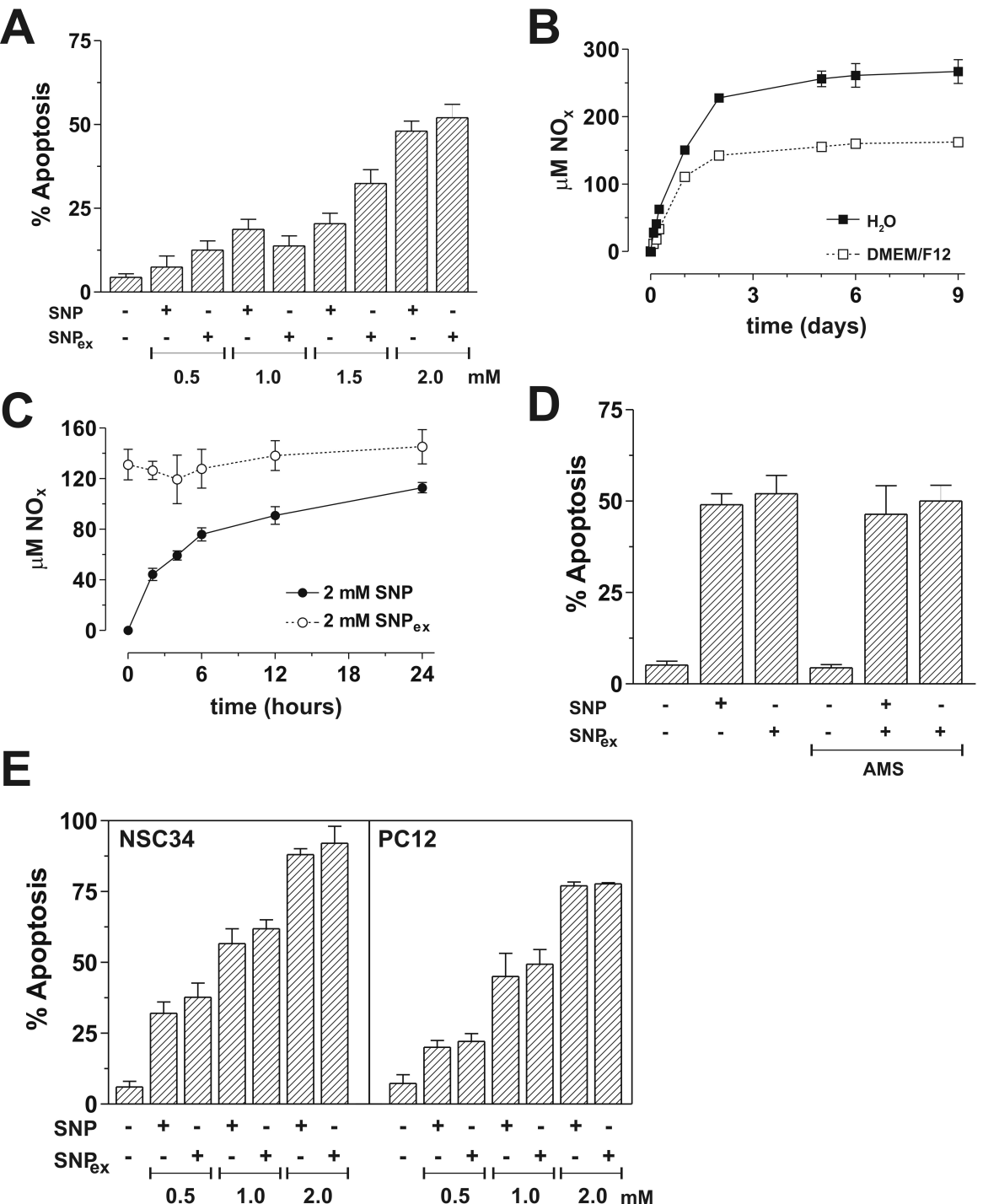
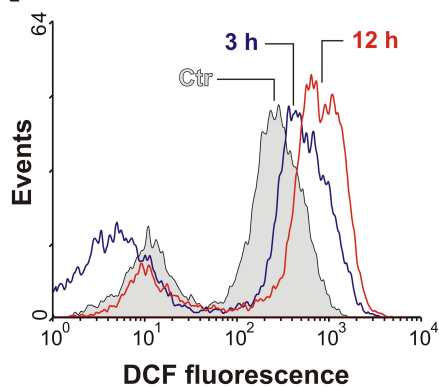
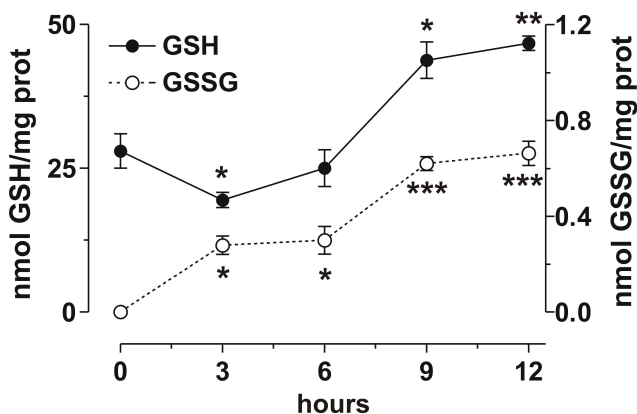
Figure 2

Figure 3

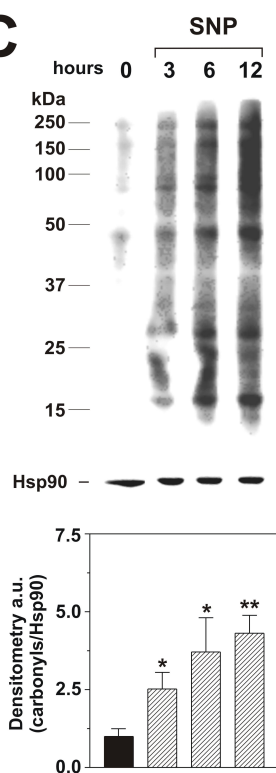
A



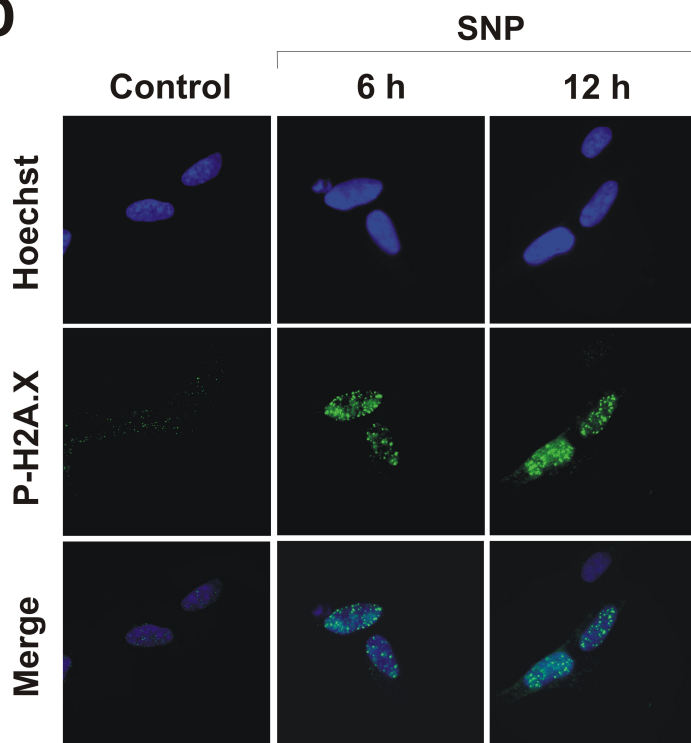
B



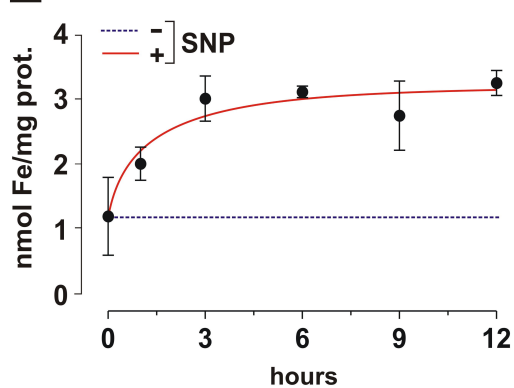
C



D



E



F

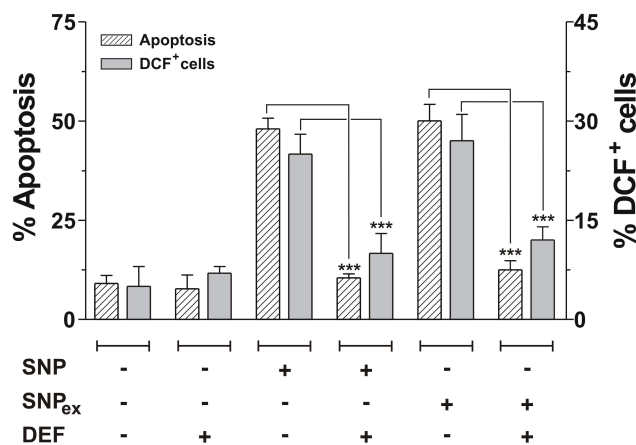
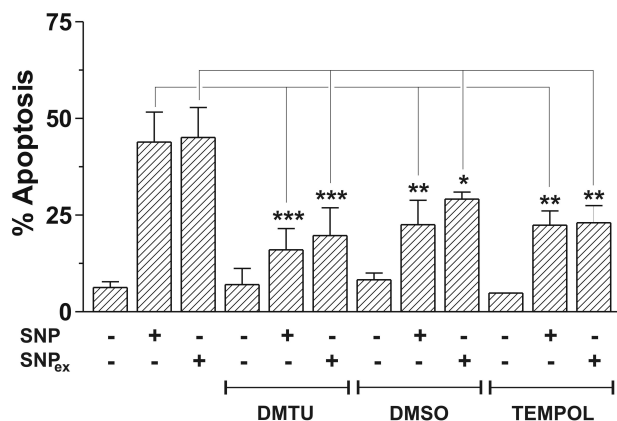
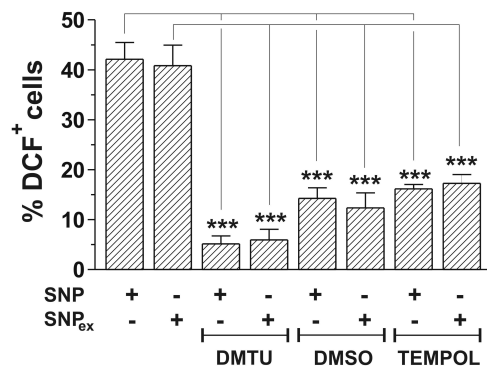


Figure 4

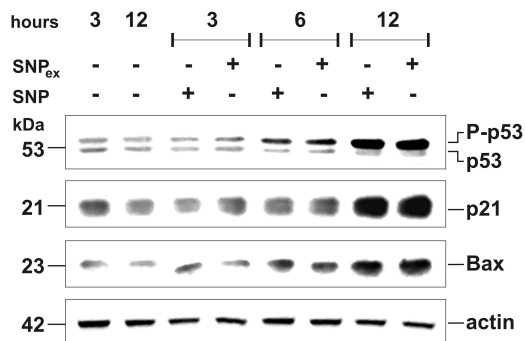
A



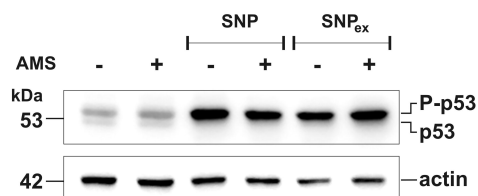
B



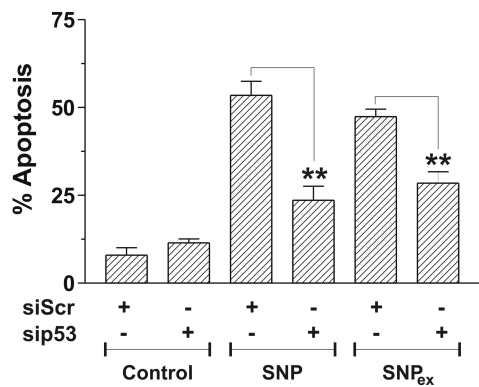
C



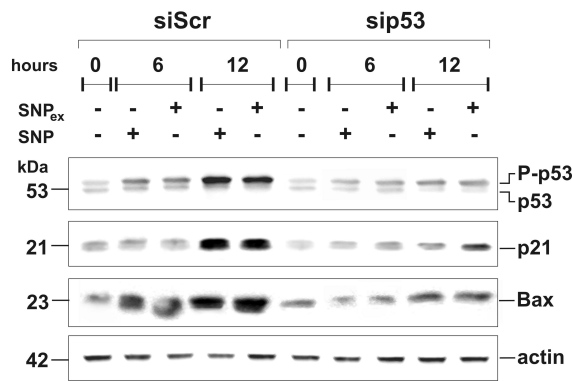
D



E



F



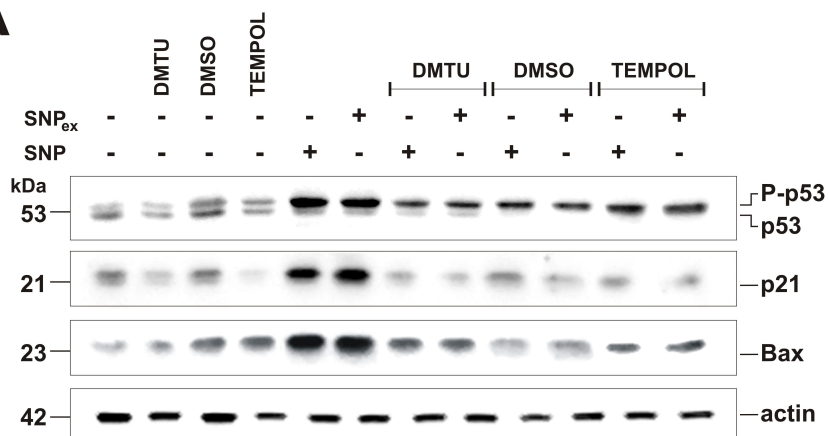
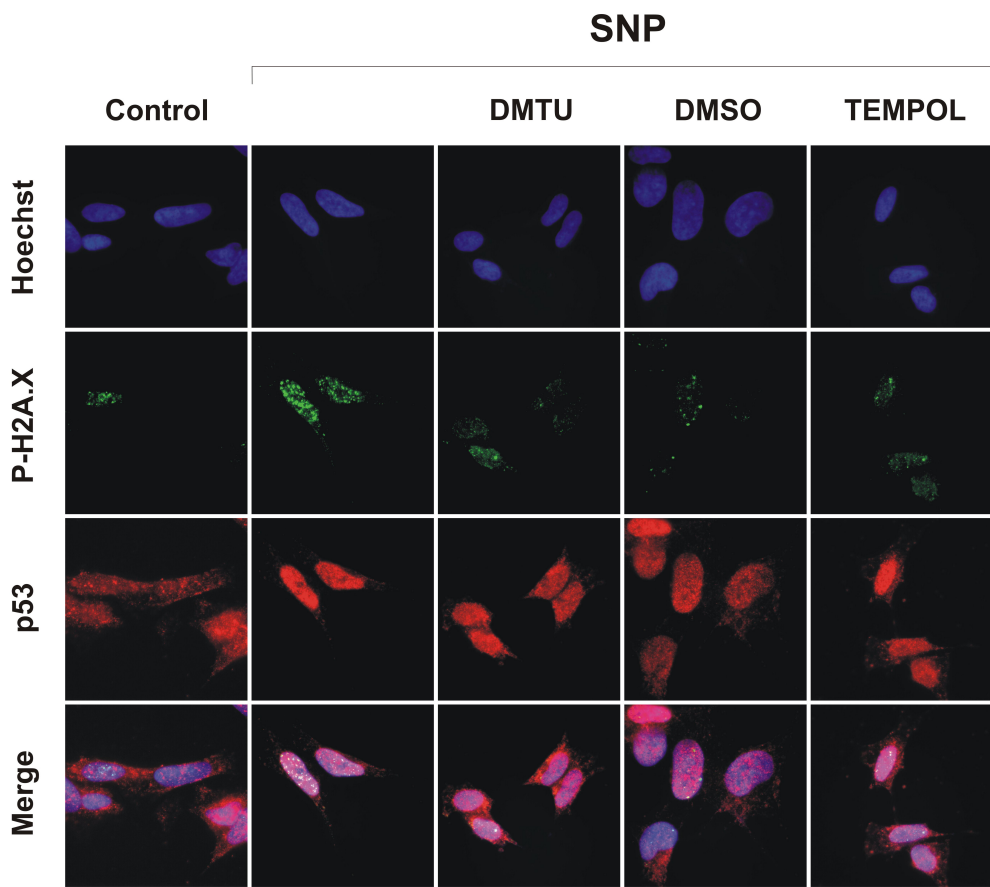
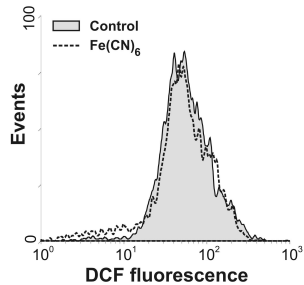
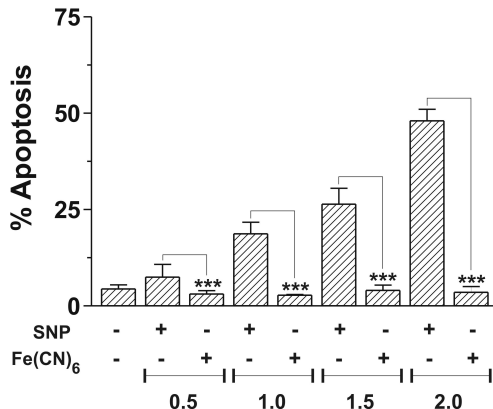
A**B**

Figure 6

A



B



C

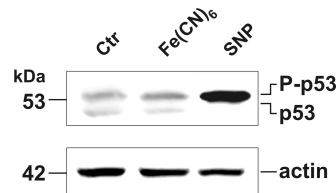
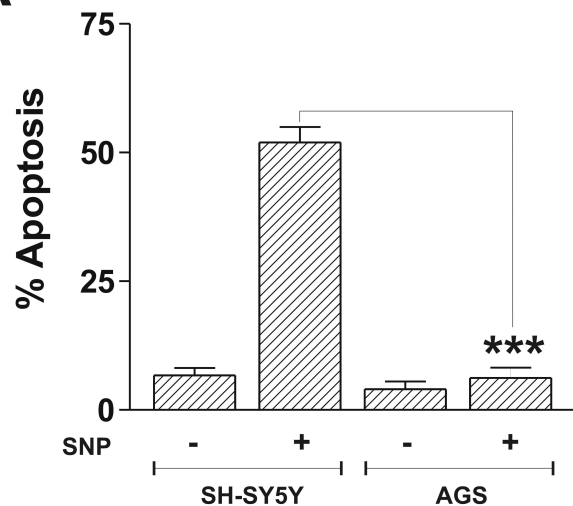
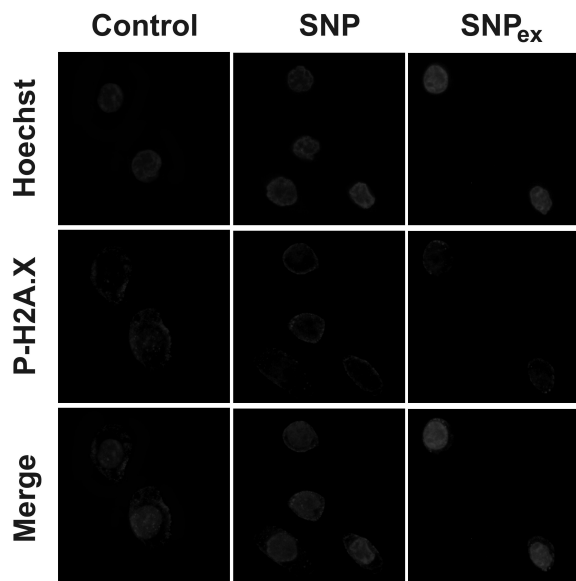


Figure 7

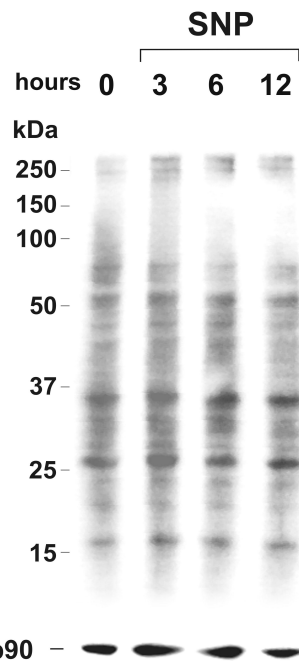
A



C



B



D

